Analysis of the ^{1}H NMR Line Shape Found in Animal Lenses

JERZY BODURKA,* GERD BUNTKOWSKY, ALEKSANDER GUTSZE, MALGORZATA BODURKA, AND HANS-HEINRICH LIMBACH

Department of Biophysics (J.B., A.G.), and Department of Physiology (M.B.), University Medical School of Bydgoszcz, ul. Jagiellonska 13, 85-067 Bydgoszcz, Poland; and Institut für Organische Chemie der Freien Universität Berlin, Takustr. 3, D-14195 Berlin, Germany (G.B., H.-H.L.)

The proton NMR line shape of rabbit lens was investigated to explain the extremely short value of the T_2^* relaxation time that determines the decay time of the lens free induction decay (FID) signal. The proton lens spectra were measured at 300 MHz, and a characteristic, antisymmetric profile was found. To determine whether the line shape is caused by unaveraged residual dipolar interaction from immobile protein protons, which would yield a homogeneously broadened line, we performed a spectral hole-burning experiment on the lens. In these experiments we could show that the line is clearly inhomogenously broadened. The inhomogeneity of the external field (ΔB_0) was excluded by comparing at room temperature (295 K) the normalized proton NMR line shape of the whole rabbit lens measured at 300 MHz with the NMR line of a reference sample of pure water of similar size and shape. The measurements of the NMR spectra of the lens cortex and nucleus alone, as well as the spin–lattice relaxation time data obtained for the lens at different frequencies, indicate that the distribution of the chemical shift values is not responsible for the lens profile. Therefore, to understand our data we have to assume that the magnetic susceptibility effect and the shape of the lens are responsible for the observed the NMR line shape and also for the short value of the T_2^* relaxation time. We calculated the magnetic field inside the lens, using the model of two concentric spheres with different susceptibilities. The results of these calculations are in very good agreement with the experimental data of the lens. The consistency of the assumed model was checked by measurements of the NMR line shapes for the lens phantom and for the lens at higher fields (500 MHz).

Index Headings: **^{1}H-NMR line shape; Rabbit lens; Hole burning; Magnetic susceptibility.**

INTRODUCTION

In recent years the technological and clinical applications of magnetic resonance imaging (MRI) have rapidly advanced.[1,2] However, it is still difficult to obtain accurate images of tissues which have a very inhomogeneous distribution of magnetic susceptibilities. The resonance frequencies of water protons at different positions in these types of tissue are shifted with respect to each other, and the resulting images are blurred.[2] Because of their implications for clinical diagnosis, the study of these effects is of great interest with respect to the application: MRI. As an example of these susceptibility effects, new data are presented, which show that the shape of the proton nuclear magnetic resonance (NMR) line of water molecules found in animal lens is caused entirely by these susceptibility effects.

The mammalian lens has a relatively simple and regular structure. It has the shape of a flattened globe, which is surrounded by a capsule, under which there is a layer of epithelial cells. These cells reproduce and create the elongated lens fibers. They are formed throughout life, and the new fibers cover the old ones. The cells lose their nuclei as they grow older.[3] The oldest fibers in the center of the lens are glued together and form a compact mass known as the nucleus. The rest of the lens forms the cortex. A normal mammalian lens contains about 65% water and 35% organic material, mainly structural protein. The lens is unique in having no blood or nerve supplies, and it exhibits, compared to other organs, only very low metabolic activities.

Lenses of different species have been studied by NMR relaxometry.[4–8] In these studies, a common spin–lattice relaxation time but two distinct spin–spin relaxation times (T_{2A}, T_{2B}) for the whole lens have been reported. In particular, a strikingly large ratio of the spin–lattice relaxation time, T_1, and the spin–spin relaxation time, T_2, was found. Moreover, the lens exhibits a rather unsymmetric line shape (Fig. 1), which resembles a shape typically found in solids more than in liquids.[9] Recently it has been shown that translational surface diffusion of bound water molecules is responsible for the spin–spin relaxation times T_{2A} and T_{2B}.[10] These short T_2 values have severely limited the investigation of the lens with a conventional MRI apparatus, as has been reported by Wu et al.[11] A detailed understanding of the physical origin of the short T_2 and also T_2^* values and the line shape found in the lens would therefore be very useful for the application of MRI to the lens. Therefore, a classical line shape analysis of the NMR spectrum of the lens combined with spectral hole-burning experiments was performed to understand the physical origin of the extremely short T_2^* value.

MATERIAL AND METHODS

We used whole lenses and fragments of several two- ($n = 4$) and four- ($n = 2$) month-old rabbits. The lenses and fragments were used for NMR measurements without any further treatments. The measurements of the line shape were performed with a Bruker MSL 300 solid-state spectrometer (at 300-MHz Larmor frequency) and a Bruker AMX-500 liquids spectrometer (at 500-MHz Larmor frequency) at room temperature. The typical 90° pulse width was 10 μs at both Larmor frequencies. The spectra were obtained as Fourier transforms of the free induction decay (FID) signal measured after a 90° pulse. The spectral hole-burning experiments[12] were done at room temperature on a home-built solid-state NMR spectrometer

Received 26 April 1996; accepted 23 July 1996.
* Author to whom correspondence should be sent.

0003-7028/96/5011-1421$2.00/0

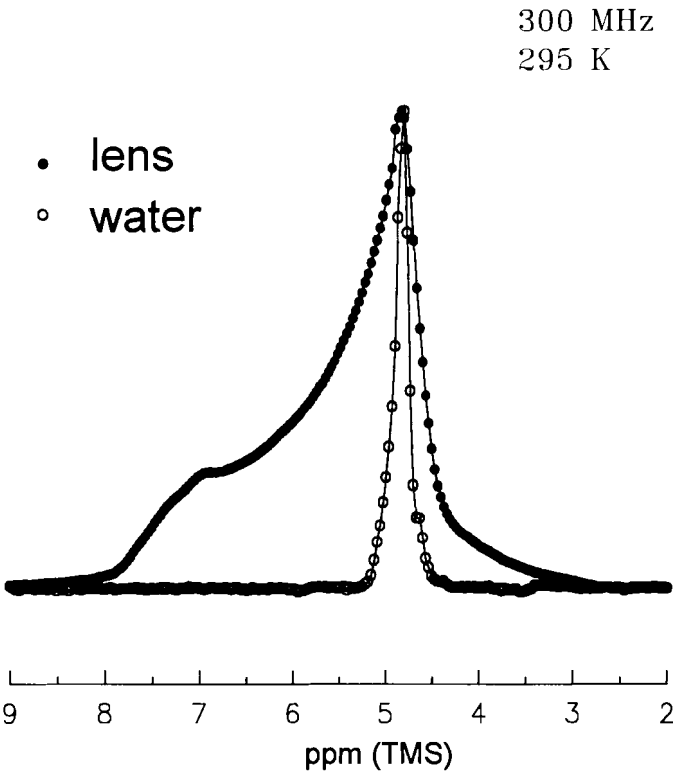

FIG. 1. The proton NMR line shape of whole rabbit lens measured at 300 MHz at room temperature (295 K). Additionally it is shown that the NMR line from a reference sample contains water. Both signals were normalized in order to compare their relative widths.

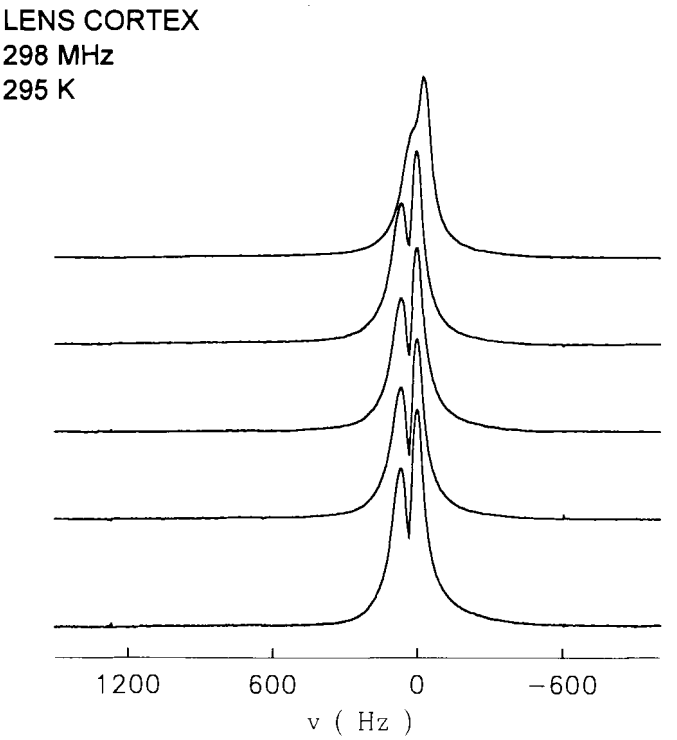

FIG. 2. The result of hole-burning experiments carried out on the lens cortex fragment at 298 MHz at room temperature (295 K). The effect of gradually increasing the duration of the soft, low-power, selective-saturation pulse is shown. The upper spectrum was measured without the saturation pulse, with the use of only the single high-power 90° detection pulse.

at 298-MHz Larmor frequency, with the use of a 1-kW Class AB amplifier, which allowed us to irradiated the sample first with a soft, low-power, selective-saturation pulse and then to irradiate with a high-power 90° detection pulse. The power of the soft pulse was adjusted by observing the width of the spectral hole in the NMR line. The experiments were performed on fragments of the cortex and of the nucleus of the lens. Additionally, a lens phantom was prepared. The phantom was made by immersing a small glass sphere filled with water (which serves in this case as the nucleus) in the homogenates obtained from the whole rabbit lens. The NMR spectra of the phantom were measured at 300 MHz at room temperature.

RESULTS AND DISCUSSION

As is well known from the literature about solid-state NMR,[10,13] there exist different types of line-broadening mechanisms, in particular, homogeneous and inhomogeneous line broadening. As was mentioned above, the observed line shape for the lens resembles a powder-like structure, which looks similar to the lines observed in solid samples, where unaveraged magnetic dipolar interactions among the protons govern the spectrum,[11] leading to a homogeneous broadening of the line. While the dipolar couplings are fully averaged in normal liquids, residual dipolar interactions could arise from couplings among protein protons, because these crystallins are relatively immobilized at physiological concentrations.[14,15] It has been discussed in the literature how their line shape can be transferred to both water and protein protons by—compared with the spin–lattice relaxation rate ($1/T_1$)—rapid magnetization transfer, which also exists at high fields.[16,17] If such a mechanism determines the spectrum, the observed line should be a homogeneously broadened line with a generally complex line shape. Such a line would, in general, exhibit exponential spin–lattice relaxation and nonexponential spin–spin relaxation behavior.[17] To analyze whether the observed line shape (Fig. 1) is caused by a homogenous broadening mechanism, we performed a spectral hole-burning experiments on the lens. The idea of the experiments is to saturate the sample with a long, low-power radio-frequency (rf) pulse, whose spectral width is much smaller than the linewidth. This pulse either would selectively saturate only a small part of the line, i.e., burn a spectral hole[12] (inhomogeneous broadening), or would saturate the whole line (homogeneous broadening). The results of the "hole-burning" experiments on the lens and on the cortex are shown in Figs. 2 and 3, which prove that the line shapes of the lens cortex and the lens nucleus and thus also of the whole lens are inhomogenously broadened.

As was pointed elsewhere, there exist different mechanisms for explaining this inhomogenous broadening: (1) inhomogeneity of the external magnetic field (ΔB_0); (2) distribution of chemical shift values, either because of differences in the local chemical environment of the water molecules or because of anisotropic reorientations, leading to residual chemical shielding anisotropy; or (3) magnetic susceptibility effects.

The first possibility can be excluded by Fig. 1, which compares the normalized room-temperature (295 K) pro-

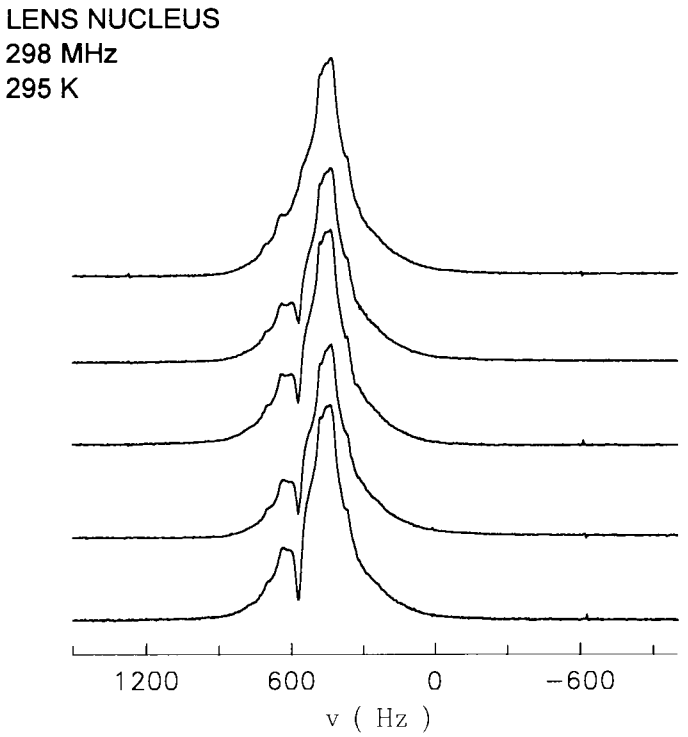

FIG. 3. The result of hole-burning experiments carried out on the lens nucleus fragment at 298 MHz at room temperature (295 K). As in Fig. 2, the effect of gradually increasing the duration of the soft, low-power, selective-saturation pulse is shown. The upper spectrum was measured without the saturation pulse, with the use of only the single high-power 90° detection pulse.

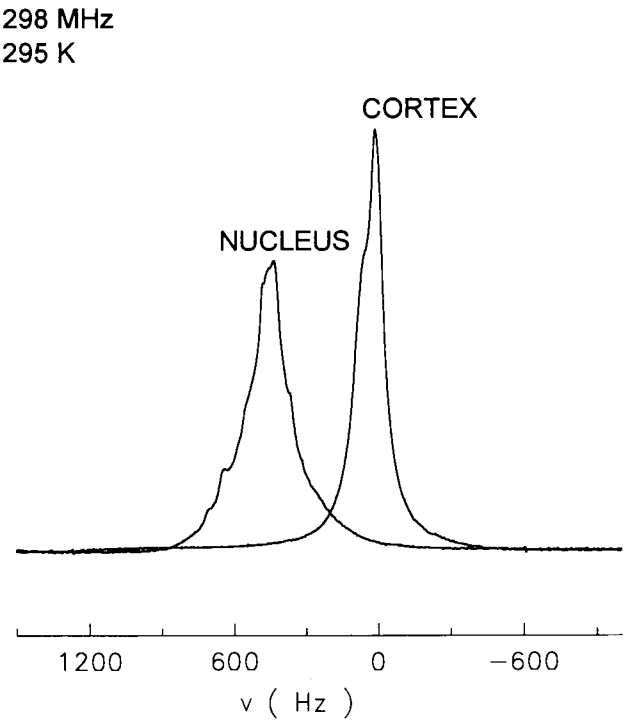

FIG. 4. The proton NMR line shapes of the lens cortex and the nucleus fragments measured at 298 MHz at room temperature (295 K). Both signals were normalized.

ton NMR line shape of the whole rabbit lens measured at 300 MHz with the NMR line of a reference sample of pure water of similar size and shape. The half-width of the water line (~30 Hz) is a measure of the external magnetic field inhomogenity (ΔB_0). It is much lower than the half-width of the lens (~500 Hz). Therefore, the external magnetic field inhomogenity is not responsible for the observed linewidth.

To decide between the other two possibilities, we separated the nucleus and the cortex of the lens and measured them alone. The results of such measurements are shown in Fig. 4. In the case where the line shape is governed by a distribution of chemical shift values, the sum of the two spectra should reproduce the shape of the whole lens, while in the case of susceptibility effects, the sum of the two spectra would not reproduce the shape of the NMR spectrum of the whole lens. Additionally the dependence of the spin—lattice relaxation time (T_1) upon the Larmor frequency (ν_L) for the rabbit lens is opposite the case of the anisotropic chemical shift relaxation; namely, T_1 becomes longer when ν_L increases.[9] Therefore, the experimental findings show (Fig. 4) that the latter case—namely, a change in the magnetic susceptibility—is responsible for the observed NMR spectra of the whole lens.

THE LENS MODEL

To analyze the susceptibility effect in detail, we calculated the magnetic field inside the lens. As was mentioned above, the lens itself consists of two parts: an inner part (i.e., the nucleus) and an outer shell (i.e., the cortex). In an effort to simplify the magnetic field calculations, the lens was modeled by two concentric spheres of different susceptibility with a step in the susceptibility at the boundary from the inner to the outer sphere. The inner sphere is attributed to the nucleus, and the outer shell is attributed to the cortex (Fig. 5).

With the application of an external homogeneous static magnetic field, H_0, the spherical symmetry of the problem is reduced to a cylindrical symmetry, where the direction of H_0 pointing through the center of the spheres determines the axis of symmetry. Therefore, the system is most easily solved by using spherical polar coordinates (r, θ, ς) with the z-direction pointing in the direction of the external magnetic field.

There are no electric currents inside the sample; therefore the rotation of the magnetic field is zero (rot H = 0), and H can be described as the gradient of a scalar potential ϕ (Eq. 1) which obeys the Laplace equation (Eq. 2),[18] i.e.,

$$H = -\text{grad}(\phi) \tag{1}$$

and

$$\Delta\phi = 0. \tag{2}$$

Using the Fourier method, we may obtain a solution of the Laplace equation[18] that gives us the distribution of the magnetic scalar potential in the cortex and the nucleus. Next, from Eq. 1 the magnetic fields inside the nucleus (H_N) and inside the cortex (H_C) can be calculated. The magnetic induction for an isotropic medium filling the nucleus (B_N) and in the cortex (B_C) is calculated from the relation $B_\nu = \mu_\nu \mu_0 H_0$; where ν = C, N. Inside the nucleus the magnetic induction is homogeneous with a value of

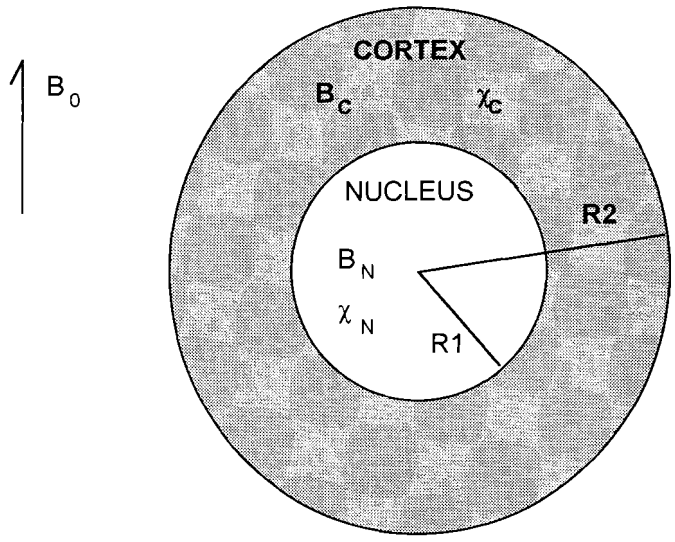

FIG. 5. The schematic representation of the lens model used in the magnetic field calculations. It was assumed that the lens shape is spherical with the radii $R2$. The inner concentric sphere with the radii $R1$ is attributed to the lens nucleus. This sphere is filled with diamagnetic material with magnetic susceptibility χ_N. The outer spherical shell, with thickness determined by $R2 - R1$, forms the cortex. The cortex is filled with diamagnetic material with magnetic susceptibility χ_C. The whole lens model is placed into the constant external magnetic field B_0, and the magnetic inductions in the cortex and the nucleus are given by B_C and B_N, respectively.

$$B_N = \frac{9\mu_N\mu_C}{\mu_C(6 + 3\mu_N) + 2(1 - s)(\mu_C - \mu_N)}B_0 \qquad (3)$$

where $s = (R1/R2)^3$, μ_N and μ_C are the magnetic permeabilities, and $R1$ and $R2$ are the radii of the nucleus and the lens, respectively. In the cortex, the magnetic induction is a function of the position. In spherical polar coordinates, $B_C(r, \theta)$ is given by the following expression:

$$B_C = \frac{3\mu_C(2\mu_C + \mu_N) - \left(\frac{R1}{r}\right)^3 \mu_C(\mu_C - \mu_N)\left(\cos^2(\theta) - \frac{1}{3}\right)}{3\mu_C(2 + \mu_N) + 2(1 - s)(\mu_C - \mu_N)(\mu_C - 1)}B_0. \qquad (4)$$

It is interesting to note that, if the condition $\mu_N = \mu_C$ holds, then both equations give the well-known results for the magnetic induction of a solid sphere placed in an external dc field B_0.[18] Using the relation $\mu_v = 1 + \chi_v$ and with $|\chi_v| \ll 1$ and v = N, C, and keeping only the first terms in the Taylor series of Eqs. 3 and 4, one obtains for the nucleus:

$$B_N \cong \left(1 + \frac{2}{3}\chi_N\right)B_0 \qquad (5)$$

and for the cortex:

$$B_C = \left(1 + \frac{2}{3}\chi_C\right)B_0 - \left(\frac{R1}{r}\right)^3(\chi_C - \chi_N)\left(\cos^2(\theta) - \frac{1}{3}\right)B_0. \qquad (6)$$

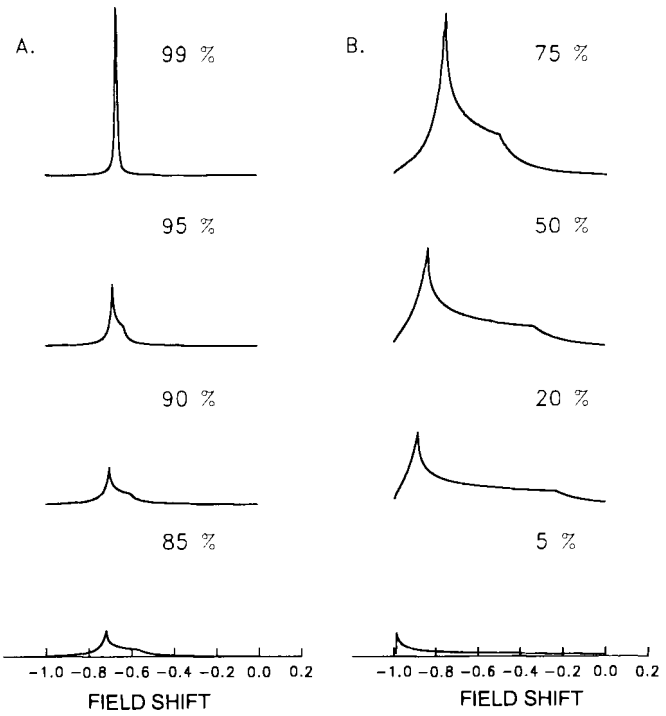

FIG. 6. The calculated histograms from Eq. 6 of the spherical shell filled with water ("air bubble"). The effect of changing the relative air volume of the "air bubble" is shown. The number 99% signifies the relative water volume, whereas 1% of the total volume is occupied by the air. Histograms in column **A** and **B**, respectively, are drawn in the same scale, whereas the scale of histograms from the **B** column is 10 time smaller than the **A** scale.

Equation 5 shows that the magnetic induction in the nucleus is uniform, whereas in the cortex it depends on r and θ. The normalized field shift $(\Delta B)_n$ is given by

$$(\Delta B)_n = \frac{\Delta B}{B_0|\chi_v|} \qquad (7)$$

where v = N, C.

As was discussed by Durney et al., it is convenient to describe the changes of the magnetic field due to a magnetic material in terms of a histogram[19] where the number of points N having a given field shift ΔB is plotted against ΔB. The histogram is equivalent to the line shape without spin–spin broadening. For a solid sphere, we obtain a single spike at $(\Delta B)_n = -2/3$, since the field in the nucleus is uniform. From Eq. 6 we can calculate the well-known result of Durney and co-workers for the "air bubble" that they used for modeling lung tissue.[19,20] Assuming that the nucleus is filled with air and the cortex is filled with water, we obtain as a result:

$$(\Delta B)_n = -\frac{2}{3} + \left(\frac{R1}{r}\right)^3\left(\cos^2(\theta) - \frac{1}{3}\right). \qquad (8)$$

We used the above equation to calculate the histogram for a spherical shell of water. Integration over the whole shell volume gives the complete histogram. The results of such calculations are shown in Figs. 6 and 7. The calculated histograms (essentially the same as in the Durney work[19]) clearly resemble (especially those for the 15–30% volume occupied by the nucleus) the observed proton NMR line shape of the lens. However, the lens nu-

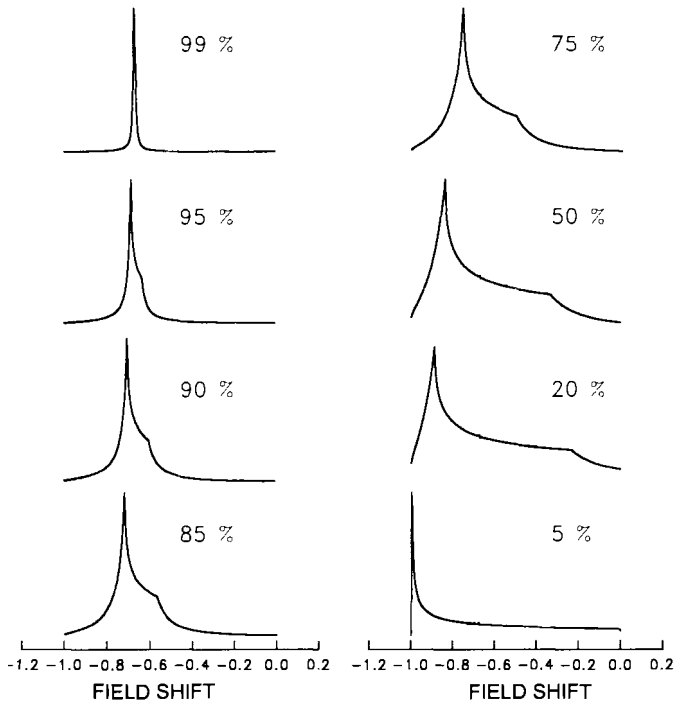

FIG. 7. The calculated histograms from Eq. 6 of the spherical shell filled with water ("air bubble"). All histograms were normalized. The effect on the histogram shape from changing the relative air volume is shown.

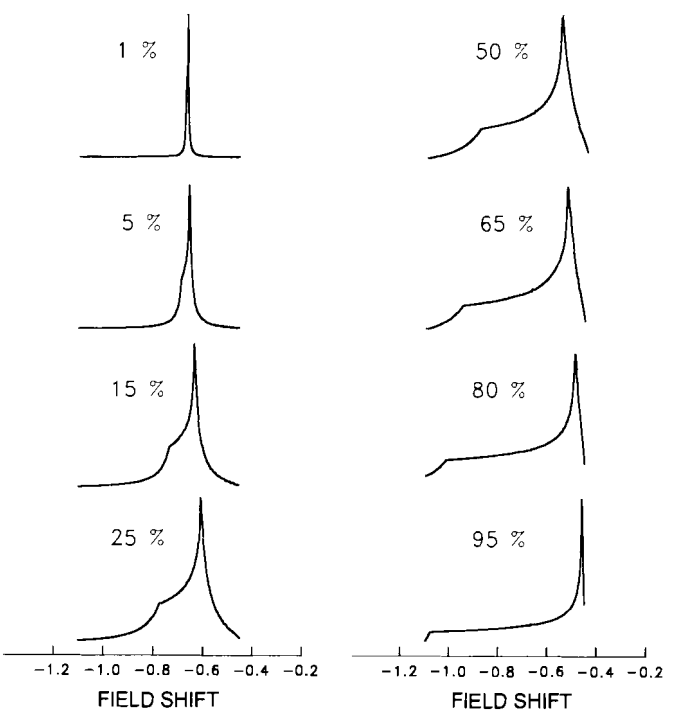

FIG. 8. The calculated histograms from Eq. 9 of the lens model. All histograms were normalized. The effect of changing the relative nucleus volume when the parameter k is fixed ($k = -0.7$) is shown. The number 1% signifies the relative nucleus volume, whereas 99% of the total volume is occupied by the cortex. The position of the maximum line intensity is shifted in the direction of the higher fields when the relative nucleus volume increases.

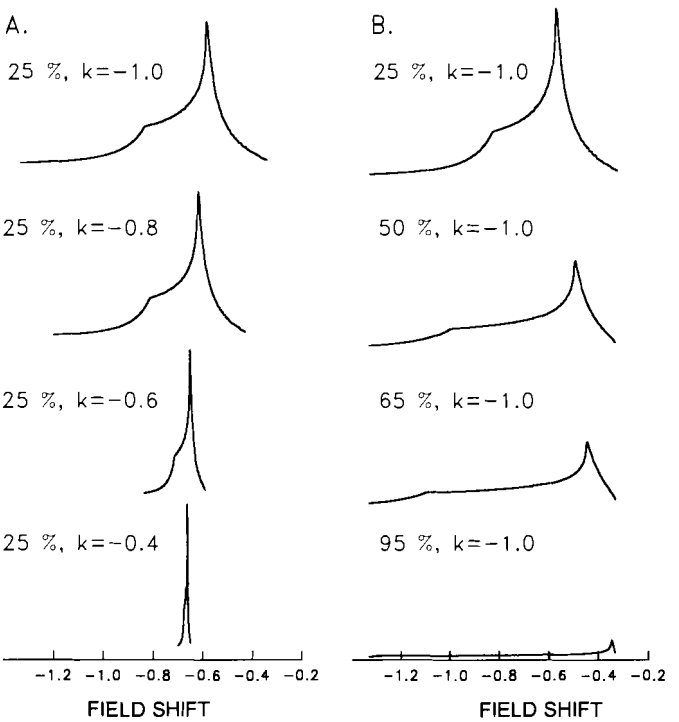

FIG. 9. The calculated and normalized histograms from Eq. 9 of the lens model. In the column marked **A**, the effect of changing of the parameter k when the relative nucleus volume is fixed is shown. Note that the maximum line intensity is shifted in the direction of the lower fields when k increases. In the column marked **B**, the effect of changing the relative nucleus volume when k is fixed ($k = -1$) is shown. The position of the maximum line intensity is shifted in the direction of the higher fields when the relative nucleus volume increases.

cleus is filled with diamagnetic material (diamagnetic water proteins solution), whereas in the lung tissue model the nucleus was filled with air, which is the paramagnetic material. The condition for the magnetic susceptibility of the nucleus and the cortex determines their relative positions in the NMR spectrum. According to this assumption, the nucleus spectra should appear at lower field in comparison to the position of the cortex. This situation is reflected in Fig. 4, where the experimental line shapes for the two lens fragments are shown. Comparing Eqs. 6 and 8, we have found that, if the condition $\chi_C > \chi_N$ holds, then histogram broadening appears in the direction of decreasing field shift. Therefore, for the lens histogram broadening appears, in contrast to the air bubble, in the direction of decreasing field shift.

Now Eq. 6 may be rewritten as follows:

$$(\Delta B)_n = -\frac{2}{3} + k\left(\frac{R1}{r}\right)^3\left(\cos^2(\theta) - \frac{1}{3}\right) \qquad (9)$$

where $k = 1 + \chi_N/|\chi_C|$.

With the use of this equation, we may calculate the histogram for the outer shell (cortex) of the lens model. The results of these calculations are shown in Figs. 8 and 9. Note that the position of the line maximum depends on a relative volume of the nucleus as on k. Increasing the nucleus volume causes a shift to higher fields, while increasing k causes a shift to lower field. For a relative nucleus volume between 25% and 35% and $k = -1$, the obtained histograms are very similar to the observed lens

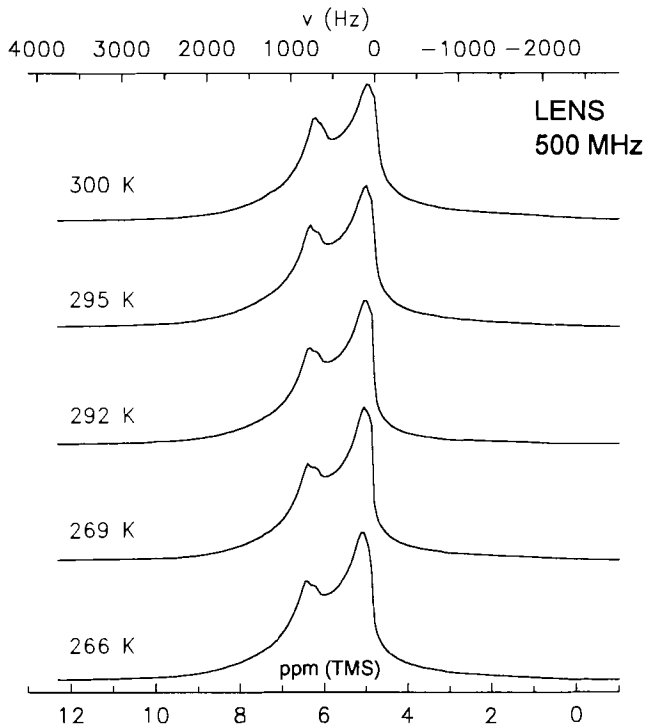

FIG. 10. The proton NMR spectra of rabbit lens measured at 500 MHz as a function of temperature.

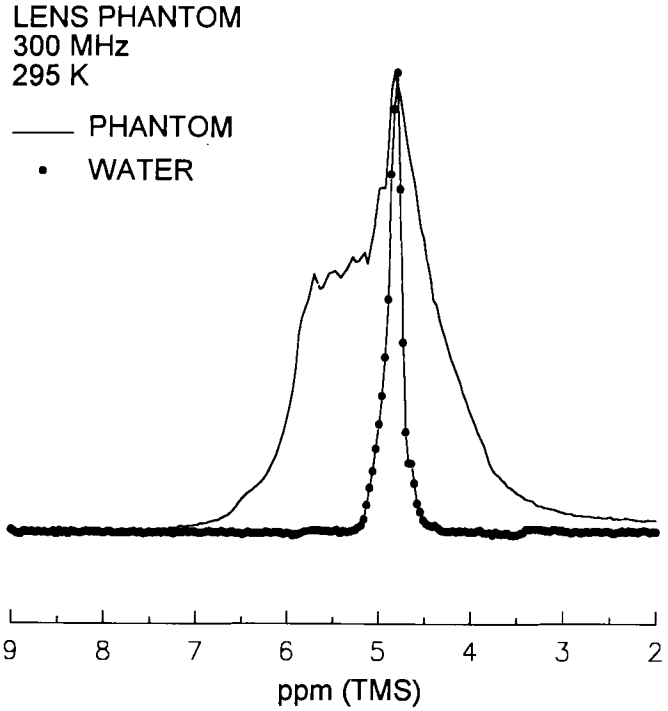

FIG. 11. The proton NMR line shape of the lens phantom measured at 300 MHz at room temperature (295 K). Additionally, it is shown that the NMR line of the reference sample contains water. Both signals were normalized in order to compare the relative widths and line positions.

spectra (Fig. 1). The value of $k = -1$ and the value of $\Delta\chi_{CN} = \chi_C - \chi_N \cong 3\ 10^{-6}$ obtained from Eq. 5 and Fig. 4 allow us to tentatively evaluate the values of magnetic susceptibilities for the nucleus, $\chi_N = -6\ 10^{-6}$, and the cortex, $\chi_C = -3\ 10^{-6}$. However, these values can be overestimated, because the exact volume occupied by the nucleus is not precisely known. It should be noted, however, that the NMR spectrum of the whole rabbit lens simultaneously contains contributions of the cortex and nucleus. The position of the nucleus line is close to the maximum of the cortex line and cannot be resolved separately at 300 MHz. The relative difference between the position of the nucleus and the cortex maximum increases (according to Eqs. 5 and 6) with an increase in the external magnetic field. Therefore, we measured the NMR spectra of the lens at 500 MHz using the rabbit lens of a four-month-old animal (larger volume occupied by the nucleus) to "uncover" the nucleus signal. The results are shown in Fig. 10. Evidently the second pike observed at about 6.5 ppm results from the NMR nucleus signal.

We also performed measurements of the NMR line shape of the lens phantom. The NMR spectra for the phantom and the water reference signal are shown in Fig. 11. The characteristic line shape found for the phantom is very similar to the lens. Therefore, it results from inhomogenously broadening caused by the shape of the sample and the magnetic susceptibility effect.

CONCLUSION

The NMR line shape found for rabbit lens resembles a powder-like structure. To determine whether the line shape is caused by unaveraged residual dipolar interaction from immobile protein protons, which would yield a homogeneously broadened line, we performed spectral hole-burning experiments on the lens. In these experiments we could show that the line shape is clearly inhomogeneous. Therefore, the shape of the line has to be attributed either to a distribution of the chemical shift values or to a magnetic susceptibility effect. To decide between these two possibilities, we separated the nucleus and cortex of the lens, and measured each alone. In the first case, where the line shape is governed by a distribution of chemical shift values, the sum of two spectra should reproduce the shape found in the intact lens, in contrast to the second case, where the sum of two spectra would not reproduce the shape of the whole lens. The experimental findings showed that a change of the magnetic susceptibility is responsible for the line shape. To get a quantitative picture of these effects, we calculated the magnetic field inside the lens, using the model of two concentric spheres with different susceptibilities. The results of these calculations are in very good agreement with the experimental data of the lens and of the lens phantom. Thus we can show that the proton NMR line shape of water molecules found in animal lens is caused by susceptibility effects, which are also responsible for the extremely short T_2^* value.

ACKNOWLEDGMENT

This work was supported by Polish KBN Program 4 PO5A 015 10.

1. C. B. Higgins, H. Hedvig, and C. A. Helms, *Magnetic Resonance Imaging of the Body* (Raven Press, New York, 1992).
2. J. M. S. Hutchison, "NMR Proton Imaging", in *Magnetic Resonance in Medicine and Biology* M. A. Foster, Ed. (Pergamon Press, Oxford, 1985), p. 157.
3. H. Maisel, *The Ocular Lens: Structure, Function, and Pathology* (Marcel Dekker, New York, 1985).

4. P. Racz, K. Tompa, and I. Pocsik, Exp. Eye Res. **29,** 601 (1979).
5. S. Lerman, Lens Eye Tox. Res. **8,** 121 (1991).
6. P. J. Stankiewicz, K. R. Metz, J. W. Sassani, and R. W. Brigs, Invest. Ophthalmol. Vision Sci. **30,** 2361 (1989).
7. A. Gutsze, J. A. Bodurka, R. Olechnowicz, and A. Jesmianowicz, Colloids Surf. A: Physicochem. Eng. Aspects **72,** 295 (1993).
8. J. Bodurka, A. Gutsze, G. Buntkowsky, and H. H. Limbach, "The Investigation of Dynamics of Water Molecules in Normal and Dehydrated Rabbit Lens Based on NMR Measurements", in *Magnetic Resonance and Related Phenomena,* extended abstracts of the XXVIIth Congress Ampere, Kazan (1994), Vol. 1, p. 751.
9. C. A. Fyfe, *Solid State NMR for Chemists* (C.F.C. Press, Guelph, Ontario, Canada 1983).
10. J. Bodurka, G. Buntkowsky, A. Gutsze, and H. H. Limbach, Z. Naturforsch. **51c,** 81 (1996).
11. J. C. Wu, E. C. Wong, E. L. Arrindel, K. B. Simons, A. Jesmanowicz., and J. S. Hyde, Invest. Ophthalm. Visual Sci. **34,** 2151 (1993).
12. N. Bloembergen, E. M. Purcell, and R. V. Pound, Phys. Rev. **73,** 679 (1948).
13. A. Abragam, *The Principles of Nuclear Magnetism* (Oxford, Clarendon Press, 1961).
14. C. F. Morgan, T. Schleich, G. H. Caines, and P. Farsworth, Biochemistry **28,** 5065 (1989).
15. C. Beaulieu, C. L. Clark, R. D. Brown, M. Spiller, and S. H. Koenig, Magn. Res. Med. **8,** 45 (1988).
16. S. H. Koenig, R. G. Bryant, K. Hallenga, and G. S. Jacob, Biochemistry **17,** 4348 (1978).
17. S. H. Koenig, R. D. Brown, and R. Ugolini, Magn. Res. Med. **29,** 77 (1993).
18. D. J. Jackson, *Classical Electrodynamics* (Wiley, New York 1962).
19. C. H. Durney, J. Bertolina, D. C. Ailion, A. G. Cutillo, A. H. Morris, and S. Hashemi, J. Magn. Res. **85,** 554 (1989).
20. T. A. Case, C. H. Durney, D. C. Ailion, A. G. Cutillo, and H. Morris, J. Magn. Res. **73,** 304 (1987).